SERKAN ÖĞÜT[1*], HASAN KAYA[2], AYKUT KENTLI[1], KERIM ÖZBEYAZ[1],
MEHMET ŞAHBAZ[3], MEHMET UÇAR[4]

INVESTIGATION OF STRAIN INHOMOGENEITY IN HEXA-ECAP PROCESSED AA7075

Severe Plastic Deformation (SPD) techniques have been used by researchers for last three decades in order to obtain Ultra-Fine Grained (UFG) materials. Equal Channel Angular Pressing (ECAP) is preferred more than other SPD techniques thanks to its high performance and practicability. Hexa Equal Channel Angular Pressing (Hexa-ECAP) – modified ECAP technique which enables to apply ECAP routes for cylindrical samples properly – was preferred in this study. Within the objective of this study, the effects of coefficient and ram velocity on the mean effective strain and strain inhomogeneity of Hexa-ECAP processed Al7075 aluminium alloy were investigated. Also, the effects of ram velocity and friction coefficient on hardness homogeneity were investigated benefitting from the similarity between the hardness distribution and the strain distribution.

Keywords: Strain Inhomogeneity, Hexa-ECAP, ECAP, SPD, AA7075

1. Introduction

In the last decades, severe plastic deformation (SPD) methods have been preferred instead of conventional manufacturing methods such as rolling, forging, extrusion, in order to obtain nanostructured materials. SPD processes are defined as metal forming processes in which a very large plastic strain is imposed on a bulk process in order to obtain ultra-fine grained (UFG) metal [1]. With reference to the characteristics of polycrystalline materials, UFG materials are defined as polycrystals having very small grains with average grain sizes less than 1 μm [2]. Although there are several SPD techniques such as high-pressure torsion (HPT) [3], twist extrusion (TE) [4], accumulative roll bonding (ARB) [5], equal channel angular pressing (ECAP) is the most preferred SPD method. ECAP is a metal forming procedure in which a material is subjected to intense plastic straining but without the introduction of any change in the cross-sectional dimensions of the sample [6-9]. There are two intersecting channels in a typical ECAP die and a bulk material in billet form is subjected to force to make the billet goes through the free channel. During this process, the billet gains shear strain while it keeps dimensions constant. Thus, the process can be repeated multiple times in order to obtain a material with superior mechanical properties. In recent years, researchers have proposed modified ECAP dies like expansion equal channel angular pressing (Exp.-ECAP) die [10-11], equal channel angular rolling (ECAR) die [12] in order to increase the performance of ECAP processes. Hexagonal equal channel angular (Hexa-ECAP) die is one of these modified ECAP dies. It was proposed by Kaya [13] in order to overcome the root problem of cylindrical samples in ECAP process. Thanks to SPD methods, mechanical properties of materials such as tensile strength, fatigue strength, hardness, etc. can be improved [14-16]. In SPD processes, the microstructure and the mechanical properties of the workpiece are considerably related to the amount of strain obtained and strain homogeneity accomplished [17]. For this reason, the current tendency in the SPD studies is maximizing the effective strain induced and strain homogeneity gained. Cerri et al. [18] investigated the influence of material properties and process settings like corner angle and friction coefficient. Agwa et al. [19] obtained optimum process parameters for maximum strain homogeneity. Djavanroodi and Ebrahimi [20] investigated the effects of die parameters and material properties on magnitude and homogeneity of effective strain. Djavanroodi et al. [21] analyzed the influences of channel angle, corner angle and pass number on strain distribution behavior of ECAPed material. Basavaraj et al. [22] investigated the combined effect of geometric parameters on strain inhomogeneity and peak pressure.

[1] MARMARA UNIVERSITY, FACULTY OF ENGINEERING, MECHANICAL ENGINEERING DEPARTMENT, ISTANBUL – TURKEY
[2] KOCAELI UNIVERSITY, ASIM KOCABIYIK VOCATIONAL SCHOOL, MACHINE AND METAL TECHNOLOGY DEPARTMENT, KOCAELI – TURKEY
[3] KARAMANOĞLU MEHMETBEY UNIVERSITY, FACULTY OF ENGINEERING, MECHANICAL ENGINEERING DEPARTMENT, KARAMAN, TURKEY
[4] KOCAELI UNIVERSITY, FACULTY OF TECHNOLOGY, AUTOMOTIVE ENGINEERING DEPARTMENT, KOCAELI – TURKEY

* Corresponding author: ogutserkan@gmail.com

There are numerous studies investigating the effects of ECAP parameters on strain distribution. Although Hexa-ECAP process is a modified version of classic ECAP process, it has a distinctive design. This leads to differences in strain distribution during the process. Therefore, the effects of friction coefficient and ram velocity on the mean effective strain and strain inhomogeneity were investigated for Hexa-ECAP process in this study. Also, the parallelism between strain and hardness distribution across the diameter was shown in order to prove the relation between hardness and effective strain obtained in Hexa-ECAP process. In the experimental part of the study, a homogenized Al7075 aluminum sample was subjected to the Hexa-ECAP process. After that, hardness measurements were performed for the Hexa-ECAP processed sample. Then, a finite element model (FEM) was generated to simulate the Hexa-ECAP process of Al7075 alloy. For the validation of this finite element model, load-time curves obtained from finite element analysis and the Hexa-ECAP process were compared. After the validation step, additional finite element analyses for different ram velocities and friction coefficients were performed in order to examine the effect of these parameters on strain distribution.

2. Principles of Hexa-ECAP process

As mentioned above, Hexa-ECAP process was proposed in order to eliminate root problems in the ECAP process of cylindrical samples. Although there are numerous root applications in ECAP process, four of them are fundamental routes and can be seen in Figure 1. These routes are A, B_A, B_C and C, respectively. Applying these different routes, different slip systems can be obtained [23]. Consequently, different microstructure and mechanical properties can be obtained applying these routes. The sample is subjected to a specific value of rotation angle between each passes for the corresponding route. The sample is not subjected any rotation in route A while the sample is rotated by 90° in the alternative direction between each passes in route B_A. The sample is rotated by 90° and 180° in same directions between each passes in route B_C and route C, respectively.
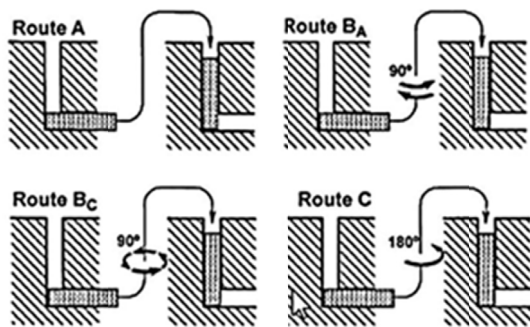

Fig. 1. Four fundamental routes applied in ECAP process [20]

These routes can be applied for square or rectangular cross-sectioned samples easily. On the other hand, applying these routes is very difficult in ECAP processes of cylindrical samples

due to the uncertainties in rotation angle. Hexa-die was designed in order to overcome this problem and its geometry can be seen in Figure 2. Unlike typical ECAP dies, there are six channels with a diameter of 20 mm in Hexa-die. During Hexa-ECAP process, four of the six channels are blocked by pins and the sample is pressed from vertical channel to horizontal channel. The pins used to block the channels were designed with half-moon end so that they could allow the sample went through them. Geometry of the pins of Hexa-die can be seen in Figure 3.
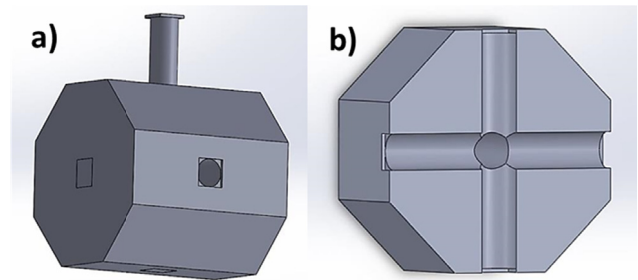

Fig. 2. a) Hexa-Die design, b) Half geometry of Hexa-Die

In Hexa-ECAP process, the sample is not ejected between sequent passes for root application. Instead, the die is rotated for desired route between each pass. Thus, it is possible to be sure of rotation angle in Hexa-ECAP process.
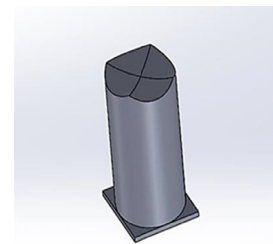

Fig. 3. Hexa-Die pin geometry

3. Experimental procedure

Al7075 alloy used in this study was supplied in a rod form with a diameter of 25 mm and length of 1000 mm. Chemical composition of the alloy can be seen in Table 1. A sample having a diameter of 19.8 mm and a length of 55 mm was machined from the billet. Before Hexa-ECAP process, the machined sample was annealed at 480°C for two hours and cooled to room temperature. After the annealing process, the annealed sample was lubricated with a layer of Molybdenum disulphide (MoS_2) in order to reduce the friction between the specimen and the die. Then Hexa-ECAP process carried out at the process temperature of 210°C and pressing speed of 1.5 mm/s. During the process, a load-time curve was obtained in order to compare with the load-time curve obtained from finite element analysis. The die used in Hexa-ECAP experiments and the processed sample can be seen in Figure 4.

TABLE 1

Chemical composition of Al7075 Alloy

Element	Al	Fe	Cu	Mn	Mg
Percent. (%)	bal.	0.22	1.59	0.11	2.53
Element	Cr	Ni	Zn	Ti	Si
Percent. (%)	0.21	0.004	5.60	0.054	0.14

After the Hexa-ECAP experiment, hardness measurements were carried out in the processed sample with load of 1000 gf for dwell time of 9s. For the measurements, TMC Measuring FM700 hardness device was used as can be seen in Figure 5.
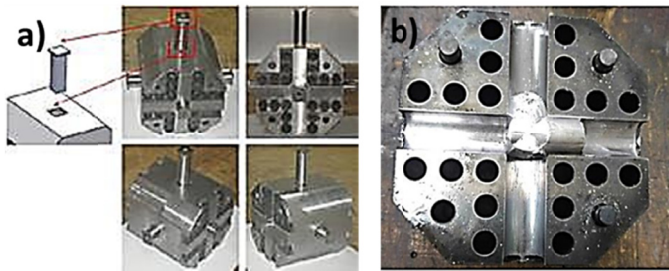

Fig. 4. a) Hexa die used in the ECAP process [12], b)Workpiece after Hexa-ECAP process

Vickers microhardness values were taken from 17 points of the measurement plane in order to compare them with effective strain values taken from finite element analysis.
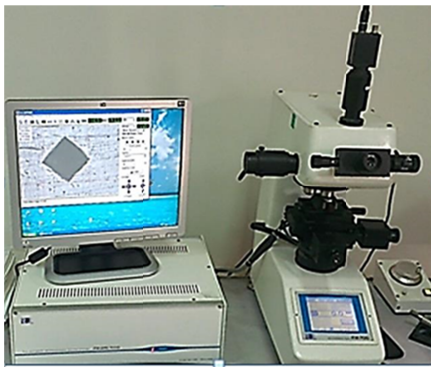

Fig. 5. Hardness Measurement

4. Simulation procedures

In this study, finite element analyses were carried out in order to numerically investigate the hardness distribution in the Hexa-ECAP Processed Al 7075 alloy numerically. Firstly, a finite element model (FEM) was generated to simulate the Hexa-ECAP process. Same boundary conditions with the ones used in the Hexa-ECAP process were applied in the FEM. The preferred element type is tetrahedral element and element number is 50000 enabling the convergence in effective strain values. The friction coefficient was taken as 0.15 so that hardness and strain values showed proximity. The generated finite element model and mesh structure of the workpiece can be seen in Figure 6.
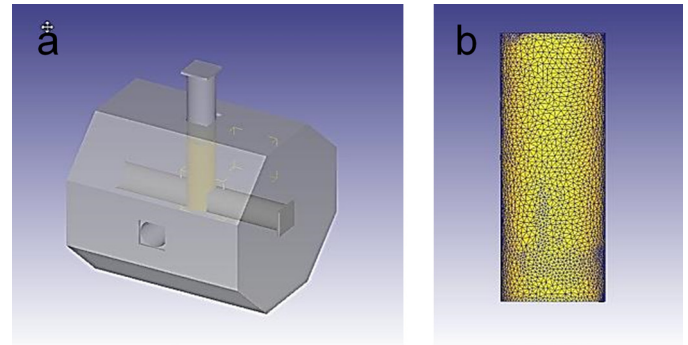

Fig. 6. a) Finite Element, b) Mesh structure of the workpiece

For the validation of the generated finite element model, the load-time curve was obtained from the simulation and it was compared with the one obtained from the experimental part of this study. This comparison can be seen in Figure 7. According to Figure 7, it is possible to say that the generated FEM was validated because of the resemblance of the trends of the two curves.

After performing the first finite element analysis, effective strain values along the diameters were calculated. Strain and hardness measurement planes can be seen in Figure 8. According to this figure, it can be seen that the same planes were used in order to collect strain and hardness data. Also, A and B points used to show the strain measurement path can be seen in Figure 8.
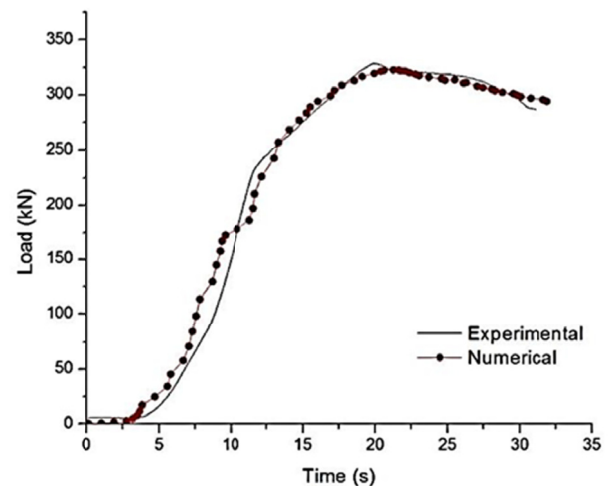

Fig. 7. Comparison between the numerical and the experimental load curves for Hexa-ECAP

After strain values were calculated, hardness and effective strain values were compared and seen that the results had same trend. The parallelism between the trend of hardness and effective strain results can be seen in Figure 9. Due to this parallelism between effective strain and hardness values, it is possible to say that there is a relation between hardness and effective strain values. Therefore, it can be assumed that the friction coefficient and ram velocity has the same effects for effective strain and hardness.

After validating the finite element model and showing the parallelism between effective strain and hardness values, 25 finite
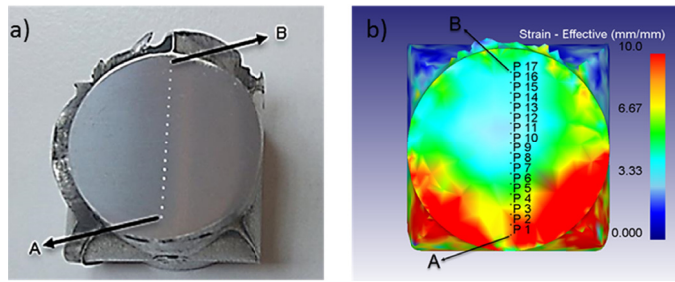
Fig. 8. a) Hardness Measurements Plane, b) Plane of Strain Measurements in FEA
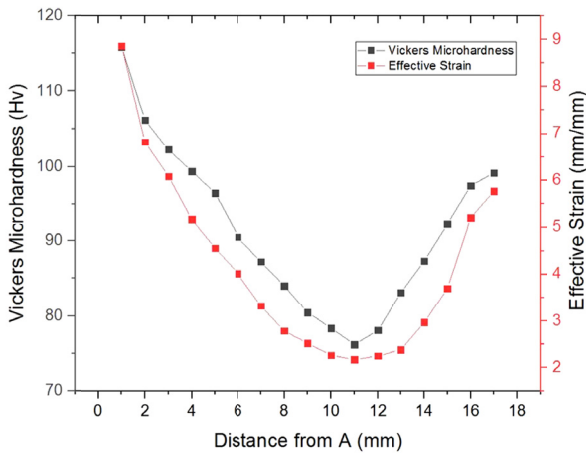

Fig. 9. Comparison between hardness value and effective strain value

element analyses were performed for different combinations of ram velocities and friction coefficients. For the ram velocity and the friction coefficient, five levels were determined. Friction coefficient and ram velocity values for each level can be seen in Table 2.

<div align="right">TABLE 2</div>

Parameters used in finite element analyses

Parameter	Levels	Values				
Ram Vel. (mm/s)	5	0.5	1	1.5	2	2.5
Friction Coeff.	5	0.05	0.1	0.15	0.2	0.25

5. Results and discussions

After 25 finite element analyses were performed, effective strain values were obtained from 17 points in the corresponding plane where hardness measurements carried out for each analysis. Mean effective strain and Variation Factor ($CV\varepsilon_p$) values were calculated for each cases to obtain strain inhomogeneity on the transverse plane. $CV\varepsilon_p$ was suggested by Zairi et al. [24] to calculate strain inhomogeneity and is as Eqn. (1):

$$CV\varepsilon_p = Stdev\varepsilon_p / Av\varepsilon_p \qquad (1)$$

where $Stdev\varepsilon_p$ is standard deviation of effective strain and $Av\varepsilon_p$ is average effective strain in the transverse plane. Increase in the

strain inhomogeneity factor means decrease in homogeneity of strain distribution. Calculated values for each analysis can be seen in Table 3.

<div align="right">TABLE 3</div>

Results obtained from finite element analyses

Analysis No.	Ram Velocity (mm/s)	Friction Coeff.	Mean Strain	$CV\varepsilon_p$
1	0.5	0.05	4.012	0.382
2	0.5	0.1	4.413	0.398
3	0.5	0.15	4.891	0.492
4	0.5	0.2	5.253	0.531
5	0.5	0.25	5.350	0.620
6	1	0.05	4.250	0.419
7	1	0.1	4.839	0.419
8	1	0.15	5.540	0.632
9	1	0.2	6.100	0.623
10	1	0.25	6.250	0.656
11	1.5	0.05	4.300	0.423
12	1.5	0.1	4.489	0.443
13	1.5	0.15	5.100	0.510
14	1.5	0.2	5.700	0.509
15	1.5	0.25	6.300	0.667
16	2	0.05	4.400	0.450
17	2	0.1	4.800	0.538
18	2	0.15	5.046	0.555
19	2	0.2	5.200	0.583
20	2	0.25	6.100	0.738
21	2.5	0.05	4.350	0.476
22	2.5	0.1	5.080	0.472
23	2.5	0.15	5.380	0.520
24	2.5	0.2	5.700	0.632
25	2.5	0.25	6.430	0.705

According to the analytical model proposed by Iawashi et al. [25] effective strain value for a typical ECAP die with channel angle of 90° and corner angle of 0° is calculated as 1.15. This value is significantly less than the mean effective strain values in Table 3. In other words, strain values obtained during Hexa-ECAP process are more than the strain value obtained by classical ECAP process. This can be attributed to the accumulated regions on the processed specimen which are being seen in Figure 10. As mentioned above, four of six channels of Hexa-Die are blocked
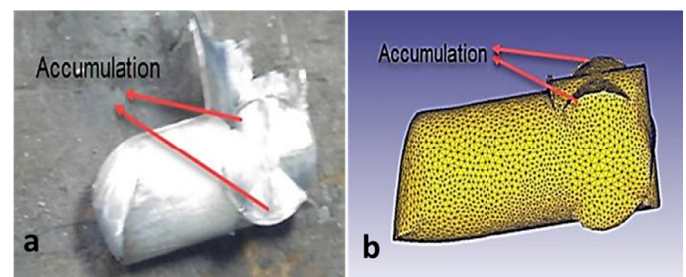

Fig. 10. a) Experimentally processed sample, b) Numerically processed sample
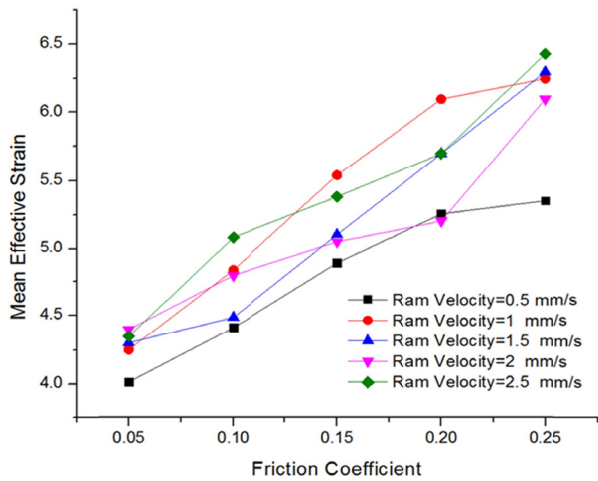
Fig. 11. Mean effective strain for different combinations of parameters

workpiece. With the increase in friction coefficient, effective strain increases at the outer surface while it does not change in inner parts. Therefore, uniformity of strain distribution decreases when the friction coefficient increases. Similar effect of friction coefficient is seen in study of Agwa et al. [19]. When the corresponding figure in this study is examined, it is observed that increase in friction coefficient causes to increase in strain inhomogeneity for ECAP process with a channel angle of 90° and a corner angle of 0°. When Figure 12 is examined from the view point of the effect of ram velocity on strain inhomogeneity, it can be deduced that the strain inhomogeneity increases in response to increasing ram velocity.

by pins with half-moon end. During the Hexa-ECAP process, the sample firstly fills the gaps between these pins. After filling these gaps, these accumulated parts proceed to horizontal channel and this situation leads to extra strain.

When Figure 11 is taken into consideration, it can be said that increment in friction coefficient causes to increase in mean effective strain. When the friction coefficient increases, strain values increase near the outer surfaces of the workpieces. Due to this increase at outer parts of the workpieces, mean effective strain value increases. Similar results can be seen in the studies of Agwa et al. [19]. According to this study, increasing friction coefficient causes to increase in average effective strain. On the other hand, it is seen that increase in ram velocity result in increase in mean effective strain especially at higher friction coefficient values which can be observed in Figure 11.

According to Figure 12, it is possible to say that strain inhomogeneity increases when the friction coefficient increases with some exceptions. In other words, increasing friction coefficient causes to decrease in strain homogeneity. This can be related to increase in effective strain at the outer surface of the
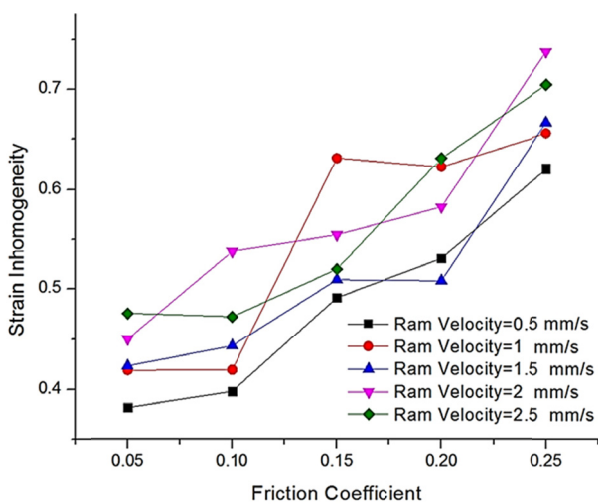
6. Conclusion

In the present study, the effect of ram velocity and friction coefficient on strain distribution was numerically investigated. The results obtained are as follow:

1. Mean effective plastic strain increases with increasing friction coefficient. On the other hand, strain homogeneity decreases due to the increasing friction coefficient.
2. Unlike friction coefficient, ram velocity has no important effect on the mean effective plastic strain and strain homogeneity.
3. Because of the parallelism between the strain and the hardness distribution, the effects of the ECAP parameters on the strain inhomogeneity are valid for the effect of these parameters on the hardness inhomogeneity.

Fig. 12. Strain inhomogeneity for different combinations of parameters

REFERENCES

[1] A. Azushima, R. Kopp, A. Korhonen, D.Y. Yang, F. Micari, G.D. Lahoti, P. Groche, J. Yanagimoto, N. Tsuji, A. Rosochowski, A. Yanagida, Severe plastic deformation (SPD) processes for metals. CIRP Annals **57** (2), 716-735 (2008). doi:10.1016/j.cirp.2008.09.005

[2] R.Z. Valiev, T.G. Langdon, Principles of equal-channel angular pressing as a processing tool for grain refinement. Progress in Materials Science **51** (7), 881 (2006). Doi:10.1016/j.pmatsci.2006.02.003

[3] A.P. Zhilyaev, T.G. Langdon, Using high-pressure torsion for metal processing: Fundamentals and applications. Progress in Materials Science **53** (6), 893-979. (2008). DOI: 10.1016/j.pmatsci.2008.03.002

[4] Y. Beygelzimer, V. Varyukhin, S. Synkov, D. Orlov, Useful properties of twist extrusion. Materials Science and Engineering: A **503** (1-2), 14-17 (2009). doi:10.1016/j.msea.2007.12.055

[5] Y. Saito, H. Utsunomiya, N. Tsuji, T. Sakai, Novel ultra-high straining process for bulk materials – development of the accumulative roll-bonding (ARB) process. Acta materialia **47** (2), 579-583 (1999). doi:10.1016/S1359-6454(98)00365-6

[6] V.M. Segal, V.I. Reznikov, A.E. Drobyshevskiy, V.I. Kopylov, Plastic metal working by simple shear. Russian Metallurgy **1**, 115-123 (1981).

[7] E. Mostaed, A. Fabrizi, D. Dellasega, F. Bonollo, M. Vedani, Microstructure, mechanical behavior and low temperature superplasticity of ECAP processed ZM21 Mg alloy. Journal of Alloys and Compounds **638**, 267-276 (2015). doi:10.1016/j.jallcom.2015.03.029

[8] Y.L. Wang, R. Lapovok, J.T. Wang, Y.S. Qi, Y. Estrin, Thermal behavior of copper processed by ECAP with and without back pressure. Materials Science and Engineering: A **628**, 21-29 (2015). doi:10.1016/j.msea.2015.01.021

[9] M.H. Shaeri, M. Shaeri, M. Ebrahimi, M.T. Salehi, S.H. Seyyedein, Effect of ECAP temperature on microstructure and mechanical properties of Al-Zn-Mg-Cu alloy. Progress in Natural Science: Materials International **26** (2), 182-191 (2016). doi:10.1016/j.pnsc.2016.03.003

[10] S. Sepahi-Boroujeni, F. Fereshteh-Saniee, Expansion equal channel angular extrusion, as a novel severe plastic deformation technique. Journal of Materials Science, **50** (11), 3908-3919 (2015). doi: 10.1007/s10853-015-8937-9

[11] S. Sepahi-Boroujeni, F. Fereshteh-Saniee, The influences of the expansion equal channel angular extrusion operation on the strength and ductility of AZ80 magnesium alloy. Materials Science and Engineering A **636**, 249-253 (2015). doi:10.1016/j.msea.2015.03.073

[12] C.Y. Nam, J.H. Han, Y.H. Chung, M.C. Shin, Effect of precipitates on microstructural evolution of 7050 Al alloy sheet during equal channel angular rolling. Materials Science and Engineering A **347** (1-2), 253-257 (2003). doi:10.1016/S0921-5093(02)00597-X

[13] H. Kaya, Eşit kanal açısal presleme (EKAP) ve yarı katı işlemle üretilen AA7075 alaşımının mikroyapı, sertlik ve yorulma davranışının incelenmesi, Kocaeli Üniversitesi / Fen Bilimleri Enstitüsü / Makine Eğitimi Anabilim Dalı, Phd Thesis, (2013)

[14] C. Haase, O. Kremer, W. Hu, T. Ingendahl, R. Lapovok, D.A. Molodov, Equal-channel angular pressing and annealing of a twinning-induced plasticity steel: Microstructure, texture, and mechanical properties. Acta Materialia **107**, 239-253 (2016). doi.org/10.1016/j.actamat.2016.01.056

[15] H. Shahmir, T. Mousavi, J. He, Z. Lu, M. Kawasaki, T. G. Langdon, Microstructure and properties of a CoCrFeNiMn high-entropy alloy processed by equal-channel angular pressing. Materials Science and Engineering: A **705**, 411-419 (2017). doi:10.1016/j.msea.2017.08.083

[16] A. Esmaeili, M.H. Shaeri, M.T. Noghani, A. Razaghian, Fatigue behavior of AA7075 aluminium alloy severely deformed by equal channel angular pressing. Journal of Alloys and Compounds **757**, 324-332 (2018). doi:10.1016/j.jallcom.2018.05.085

[17] A.V. Nagasekhar, Y. Tick-Hon, H.P. Seow, Deformation behavior and strain homogeneity in equal channel angular extrusion/pressing. Journal of Materials Processing Technology **192**, 449-452 (2007). doi:10.1016/j.jmatprotec.2007.04.093

[18] E. Cerri, P.P. De Marco, P. Leo, FEM and metallurgical analysis of modified 6082 aluminium alloys processed by multipass ECAP: Influence of material properties and different process settings on induced plastic strain. Journal of Materials Processing Technology **209** (3), 1550-1564 (2009). doi: 10.1016/j.jmatprotec.2008.04.013

[19] M.A. Agwa, M.N. Ali, A.E. Al-Shorbagy, Optimum processing parameters for equal channel angular pressing. Mechanics of Materials **100**, 1-11 (2016). doi:10.1016/j.mechmat.2016.06.003

[20] F. Djavanroodi, M. Ebrahimi, Effect of die parameters and material properties in ECAP with parallel channels. Materials Science and Engineering: A **527** (29-30), 7593-7599 (2010). doi:10.1016/j.msea.2010.08.022

[21] F. Djavanroodi, B. Omranpour, M. Ebrahimi, M. Sedighi, Designing of ECAP parameters based on strain distribution uniformity. Progress in natural science: Materials International **22** (5), 452-460 (2012). doi:10.1016/j.pnsc.2012.08.001

[22] V.P. Basavaraj, U. Chakkingal, T.P. Kumar, Study of channel angle influence on material flow and strain inhomogeneity in equal channel angular pressing using 3D finite element simulation. Journal of Materials Processing Technology **209** (1), 89-95 (2009). doi:10.1016/j.jmatprotec.2008.01.031

[23] T.G. Langdon, The principles of grain refinement in equal-channel angular pressing. Materials Science and Engineering: A **462** (1-2), 3-11 (2007) doi:10.1016/j.msea.2006.02.473

[24] F. Zaïri, B. Aour, J.M. Gloaguen, M. Naït-Abdelaziz, J.M. Lefebvre, Numerical modelling of elastic-viscoplastic equal channel angular extrusion process of a polymer. Computational Materials Science **38** (1), 202-216 (2006). doi:10.1016/j.commatsci.2006.02.008

[25] Y. Iwahashi, Z. Horita, M. Nemoto, T.G. Langdon, An investigation of microstructural evolution during equal-channel angular pressing. Acta Materialia **45** (11), 4733-4741 (1997). doi:10.1016/S1359-6454(97)00100-6